

Jun Wang¹, Sundar A. Christopher¹, Jiyoun Kim², Fred Brechtel³¹Department of Atmospheric Sciences, University of Alabama in Huntsville, Huntsville, AL, 35805²Meteorological Research Institute, Seoul, Korea³Brechtel Manufacturing Inc., Hayward, CA 94544

1. INTRODUCTION

The significance of aerosols in the climate system has been emphasized in many recent studies. However current quantification of aerosol forcing on climate has large uncertainties (IPCC, 2001). To fully understand the complex effect of aerosols requires an intensive measurement and analysis strategy. The emissions of natural and anthropogenic aerosols have been increasing in the past two decades due to the rapid growth of modern industry in the East Asian region. Although the abundance of aerosols in this region might have the largest aerosol forcing on climate, the understanding of aerosol properties, aerosol optical thickness (AOT) distributions and the aerosol radiative effect is poorly quantified because of limited observations and the complexity of aerosol types.

The goal of this research is to use geostationary satellite (GMS5) data, to examine the diurnal variations of aerosol properties and its corresponding shortwave (SW) radiative forcing (SWARF) in the East Asia region during the Aerosol Characterization Experiment Asia (ACE-Asia) Intensive Observation Period (IOP, April 01-April 30, 2001; Huebert et al., 1999).

2. DATA AND MODELS

The following data sets and radiative transfer models were used:

- The number size distributions measured using ground-based twin-scanning electrical mobility sizing (TSEMS) and optical particle counter (OPC) systems for dry diameters between 0.005 and 20 μm (Brechtel and Buzorius, 2001; Chun et al., 2001).
- Hourly GMS5 Visible and Infra-Red Spin Scan Radiometer (VISSR) data with spatial

resolution of 5km at nadir during ACE-Asia IOP. The VISSR has four channels, namely ch1 0.45 μm - 1.1 μm , ch2 10.1 μm - 11.5 μm , ch3 10.5 μm - 12.6 μm , and ch4 6.5 μm - 7.3 μm . In this study, ch1, ch2 and ch3 with radiometric resolution of 8 bits is used.

- The AOT inferred from Sun Photometers (SP) over nine AERONET sites (Holben et al., 1998) located in the study area (20°N-50°N, 110°E-150°E, figure 1).
- The plane parallel Discrete Ordinate Radiative Transfer (DISORT) model (Ricchiuzzi et al., 1998) is used for the creation of a lookup table (LUT) in AOT retrievals.

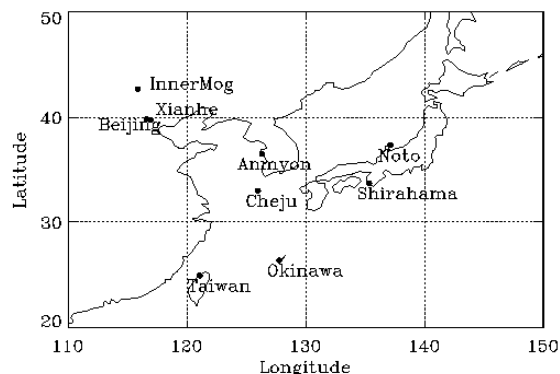


Figure 1: study area and nine Sun photometer sites used in this study.

3. METHOD

In non-cloudy conditions, the measured reflectance at the top of atmosphere (TOA) is a function of sun-satellite geometries, surface reflectance, AOT and aerosol optical properties (AOP). The AOPs in turn are determined by the particle composition, size distributions, shapes and refractive indexes. Given only one visible channel of GMS-5, to retrieve one variable (AOT), other parameters (e.g., AOP) in the retrieval algorithms must be well characterized. Also because of the complexity of aerosols in the study area, one fixed aerosol model is neither reasonable nor sufficient to model the AOPs. In this paper, a new method that dynamically incorporates ground-based AOP measurements

*Corresponding author address: Jun Wang, Dept. of Atmospheric Sciences, NSSTC, 320 sparkman drive, Huntsville, AL, 35805; e-mail:wangjun@nsstc.uah.edu

during ACE-Asia into the AOT retrieval algorithms is developed.

3.1 Aerosol Optical Model

The column aerosol size distribution is first inferred from the ground-based size distribution measurements (Brechtel and Buzorius, 2001; Chun et al., 2001). Previous studies show that aerosol size distributions can be simulated using several lognormal modes with different mode properties (d'Almeida et al., 1991). Kaufman et al (1997) summarized the global aerosol climatology and classified the aerosol into four main modes based on the aerosol radius r , $r < 0.3 \mu\text{m}$ (accumulation mode), $0.3 \mu\text{m} < r < 0.8 \mu\text{m}$ (stratospheric mode), $0.8 \mu\text{m} < r < 2.5 \mu\text{m}$ (marine salt particle mode), $r > 2.5 \mu\text{m}$ (coarse mode). Figure 2 shows the daily mean as well as the 18-day mean volume size distribution observed at the Gosan supersite during ACE Asia. Figure 2 describes a bilognormal size distribution pattern with different mode properties on different days. For a given day, the particle volume distribution can be described as:

$$\frac{dV}{d \log_{10} r} = \sum_{n=1}^2 C_n \exp \left[-\frac{1}{2} \left(\frac{\log_{10} r - \log_{10} r_{vn}}{\log_{10} \sigma_n} \right)^2 \right]$$

where subscript n indicates the mode number; r_{vn} , σ_n and C_n are the volume mean radius, standard deviation and the peak of n th mode. In this study, r_{vn} of $0.18 \mu\text{m}$ and $1.74 \mu\text{m}$, σ_n of 2.16 and 1.74 that were derived from the 18-days mean size distribution (figure 2) are used for the 1st and 2nd mode respectively. In practice, the mode peak ratio $\gamma (=C_2/C_1)$ is used in the radiative transfer calculations (Higurashi and Nakajima, hereafter HG99; Mishchenko et al., 1999) and is closely related to the Ångström exponent α . Figure 3 shows the calculated α and the single scattering albedo (ω) as a function of γ by using the derived parameters in Mie calculations assuming the refractive indexes of Patterson et al (1977). As shown in figure 3, when α and the refractive index are known, γ can be inferred and the aerosol size distribution can be determined. Thus the AOP model used in this study is not fixed but a function of α . Compared to previous algorithms (e.g., HG99) which use two AVHRR channels to retrieve α and AOT simultaneously, this study dynamically incorporates α values inferred from the SP AOTs into the retrieval process.

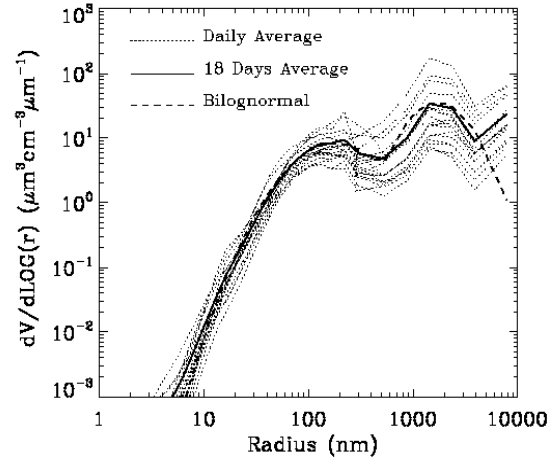


Figure 2. Volume size distribution measured in Gosan, Korea from 04/10/01 to 04/27/01, also shown is the simulated bilognormal size distribution.

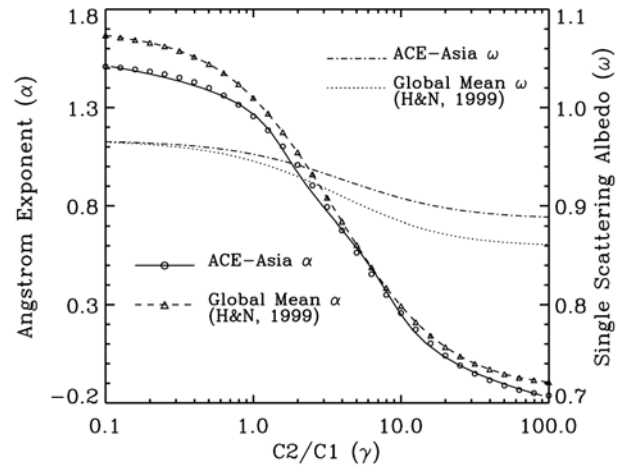


Figure3. The Ångström exponent and single scattering albedo as a function of peak ratio of bimodal size distribution in ACE-Asia and the comparison with global mean (Higurashi and Nakajima, 1999)

3.2 LUT Creation and AOT retrievals

The AOT retrievals are based on a look up table method (Wang et al., 2002, in press). The derived aerosol optical properties are used in the DISORT model to create the LUTs in which the reflectance at the top of atmosphere ρ is calculated as a function of $(\theta_0, \theta, \phi, \rho_0, \tau, \alpha)$, where θ_0, θ, ϕ are solar zenith, viewing zenith and relative azimuth angles and ρ_0 and τ are the cloud-free surface reflectance and AOT respectively. When $\theta_0, \theta, \phi, \rho_0, \alpha$ are known, the AOT can be retrieved from the GMS-inferred ρ . In this study, the ρ_0 at each GMS5 observation time period is inferred by use of minimum composite method (Wang et al., 2002, in press). A daily α map is calculated from the SP AOTs using the Barnes Successive Correction Method (SCM) (Koch et al., 1983).

The SCM is a relatively simple and widely used interpolation method that merges irregular point data from observation sites into regular grid data. To apply SCM in this study, the study area is first segmented into 16X12 grids with resolution of 2.5°X2.5°. The α at each grid is calculated using the following equation (Koch et al., 1983):

$$\alpha_i^0 = \alpha_i^b, \quad \alpha_i^{n+1} = \alpha_i^n + \frac{\sum_{k=1}^k w_{ik}^n (\alpha_{ik}^o - \alpha_k^n)}{\sum_{k=1}^k w_{ik}^n}$$

where subscript i and k represents the grid point and observation site respectively. α_i^b is the background (first guess) value at i; α_i^n is the n-th iteration estimate at i; α_k^o is the observation at k; α_k^n is the nth iteration value at grid k; w_{ik}^n is the weight of observation point k to the grid point i:

$$w_{ik} = \exp\left(-\frac{r_{ik}^2}{2R_n^2}\right)$$

where r_{ik} is the distance between i and k; R_n is the radius of influence which is changed in each iteration by $R_{n+1}^2 = \beta R_n^2$. By choosing proper values of β and R_0 , only 2~4 iterations are needed to converge $|\alpha_i^n - \alpha_i^{n+1}|$ to the desired accuracy. Let each grid has the background value (α_i^b) same as monthly mean α in its nearest AERONET site and assume the daily mean α inferred from each AERONET site as α_k^o , the daily map of α with spatial resolution 2.5°X2.5° can be produced. Future refinements will include the use of aircraft and ship measurement as well as the higher temporal resolution AERONET data. Figure 4 shows an example of the spatial distribution of α on 04/13/01 when a dust layer is leaving the east coast of China (with α as small as 0.3 showing the dominance of large particle size) and another aerosol layer near northern Japan (see also figure 5).

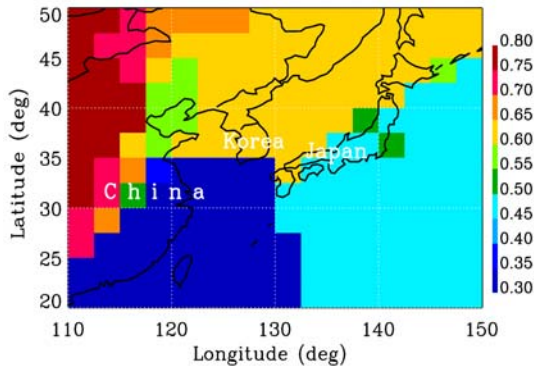


Figure 4. Derived Ångström exponent distribution on April 13, 2001.

In the next step, a aerosol detection and a cloud clearing algorithm based on the multi-channel threshold techniques are developed (Wang et al., 2002, in press). Thus, for each noncloudy pixel, we determine α from the daily α map derived from SCM method. Second, AOT is retrieved by finding the best fit between ρ and pre-calculated TOA reflectance in LUTs (which is a function of θ_0 , θ , ϕ , ρ_0 , τ , α).

4. RESULTS

Figure 5a shows a ρ visible image on 0132UTC, April 13 2001. The contrast between dust plumes and the dark ocean surface shows two aerosol layers, one was approaching Japan from the east coast of China (30°N~35°N, 120°E~130°E) and another aerosol layer was observed over North Japan (near 42°N, 140°E). The SP measurements at Cheju island (cf. figure 1) reported AOT values larger than 0.7 at 0.67 μ m in this day. The retrieved AOT map corresponding to figure 5a is shown in fig. 5b. The AOT gradient from the coast region to remote ocean is shown in figure 5b with a maximum AOT larger than 1.4 near the coast for both aerosol layers.

Figure 6 shows the comparison between the SP AOTs and ρ AOTs over Cheju Island for

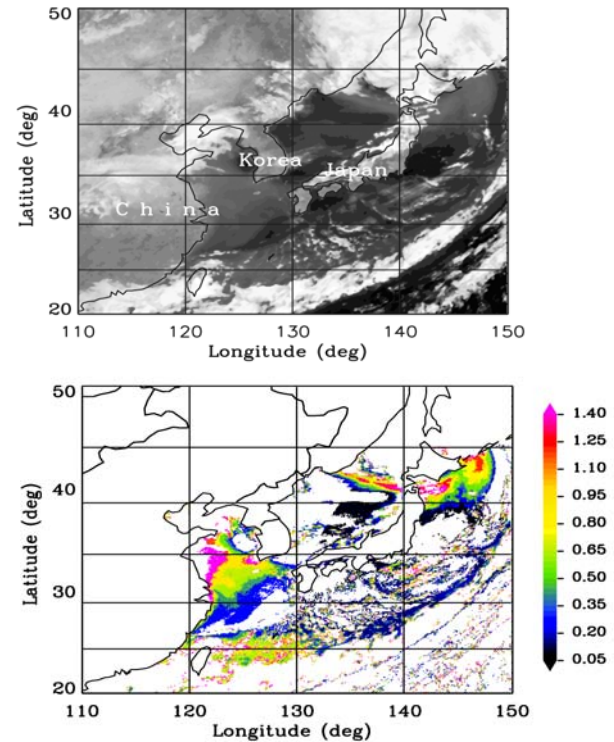


Figure 5. a) ρ visible image on 1332UTC, April 13 2001. b) the corresponding AOT distribution over ocean.

April 2002. For each comparison pair, the observation time is within 30 minutes and the 3X3 GMS pixels nearest to Cheju Island were chosen. A good correlation with a coefficient of 0.86 is found between SP and GMS retrieved AOTs. The best fit between SP and GMS AOTs shows a slight overestimation of GMS retrievals. The incorporation of Ångström exponent from aircraft measurements is under way, which will improve dynamical characterization of aerosol optical properties in our retrieval algorithms.

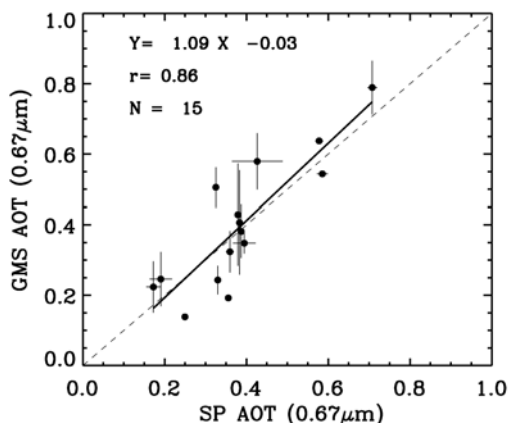


Figure 6. Comparison of GMS AOTs with the SP AOTs during ACE IOP 2001 over Cheju site. Solid line is the best fit line. The dotted line is the one-to-one line.

5. CONCLUSION

Using geostationary satellite data and AERONET derived aerosol optical thickness, an approach that dynamically incorporates ground-based measurements into the satellite AOT retrievals is demonstrated during ACE-Asia. The preliminary comparison between GMS retrieved and SP inferred AOTs shows this approach has the potential to retrieve the AOT with high temporal resolutions from geostationary satellites from one visible channel of geostationary satellites. Using the high temporal resolution aerosol optical thickness retrievals the next step is to compute the radiative effects of ACE-Asia aerosols.

Reference:

Brechtel, F. J. and G. Buzorius, 2001: Airborne observations of recent new particle formation over two urban areas in the U.S. *J. Aer. Sci.*, **32**, S115-116.

Chun, Y., J. Kim, J.-C. Choi, K.-O. Boo, M. Lee, and S.-N. Oh, Characteristic number size distribution of

aerosol during Asian dust period in Korea. *atmospheric Environment*, **35**(15), 2715-2721.

- D'Almeida G. A., P. Koepke and E. P. Shettle, 1991: *Atmospheric climatology and radiative characteristics*, A. Deepak publishing, p561.
- Kaufman, Y. J., D. Tanré, L.A. Remer, E. F. Vermote, A. Chu and B.N. Holben, 1997: Operational remote sensing of tropospheric aerosol over land from EOS moderate resolution imaging spectroradiometer, *J. Geophys. Res.*, **102**, 17,051-17,076.
- Koch, S. E., M. Desjardins, and P. J. Kocin, 1983: An interactive Barnes objective map analysis scheme for use with satellite and conventional data, *J. Climate. Appl. Meteor.*, **22**, 1487-1503.
- Higurashi, A. and T. Nakajima, 1999: Development of a two-channel aerosol retrieval algorithm on a global scale using NOAA AVHRR, *J. Atm. Sci.*, **56**, 924-941.
- Hoben, B. N., et al., 1998: AERONET- A federated instrument network and data archive for aerosol characterization, *Remote. Sens. Environ.*, **66**, 1-16
- Hubert, B., T. Bates, et al., ACE-Asia Spring 2001 Intensive Experiment Science and Implementation Plan, Draft, September 2000.
- IPCC, 2001: *Climate Change 2001: The Scientific Basis*. Contribution of Working Group I to the Third Assessment Report of the Intergovernmental Panel on Climate Change [Houghton, J. T., Y. Ding, D. J. Griggs, M. Noguer, P. J. van der Linden, X. Dai, K. Maskell, and C. A. Johanson (eds)]. Cambridge University Press, United Kingdom and New York, NY, USA, 881pp.
- Mishchenko, M. I., I. V. Geogdzhayev, B. Cairns, W. B. Rossow, and A. Lacis, 1999: Aerosol retrievals over ocean by use of channels 1 and 2 AVHRR data: sensitivity analysis and preliminary results, *Applied Optics*, **38**, 7325-7341.
- Patterson, E. M., D. A. Gillette, and B. H. Stockton, 1977: Complex index of refraction between 300nm and 700nm for Sahara aerosols, *J. Geophys. Res.*, **80**, 3,153-3,160.
- Ricchiazzi, P., S. Yang, C. Gautier, and D. Sowle, 1998: SBDART: A research and teaching software tool for plane-parallel radiative transfer in the Earth's atmosphere, *Bull. Am. Meteorol. Soc.*, **79**, 2101-2114.
- Wang, J, S. A. Christopher, J. S. Reid, H. Maring, B. N. Holben, and S. K. Yang, 2002: GOES-8 retrieval of dust aerosol optical thickness over the Atlantic ocean during PRIDE, in press, *J. Geophys. Res.*